Data Analysis and Raster Mapping of Solar Intensity Using BURT Observations

Uday Etaiwi Jallod[1], Israa Abdulqasim Mohammed Ali [2] and Kamal Mohammed Abood[1]
[1]*Department of Astronomy and Space, College of Science, University of Baghdad, 10071 Baghdad, Iraq*
[2]*Department of Remote Sensing, College of Remote Sensing and Geophysics, Al-Karkh University of Science, 10003 Baghdad, Iraq*
israa.aq88@gmail.com

Keywords: Radio Astronomy, Solar Radio Emissions, 21 Cm Hydrogen Line, Solar Intensity Contour Maps.

Abstract: From April to June of 2019, the solar hydrogen spectral line was observed with the three-meter Baghdad University Radio Telescope (BURT) using the raster scan mapping technique. This technique allowed for the production of solar intensity contour maps and its surrounding region, which emitted at the wavelength of 21 cm. The contour maps estimated by employing square windows in the sky of various sizes that involved the Sun and its surrounding area. These maps were represented in terms of solar received power, antenna temperature, and brightness temperature. The maximum values of the received power, antenna temperature and brightness temperature were obtained using an 8°×8° window of size, found to be -46 dBm, 288 K and 2300 K respectively. To investigate our results, the root mean square noise in a total power measurement was calculated for each selected window. The findings revealed that the smallest errors occurred with larger window sizes, and found to be 1×10^{-3} at window size of (8°×8°) and this gives a good indication about results accuracy. All these results showed in a good agreement with solar observations at the wavelength of 21 cm using a small radio telescope.

1 INTRODUCTION

Modern antenna systems constructed to move are commonly used in astronomical radio observation techniques. Consequently, various measurements are required to characterize the motion of the antenna power pattern in space. In radio astronomy, these measurements can be used for both continuum and spectral line observations [1]-[3]. The detection of the hydrogen emission line is particularly important among the spectral lines. Notably, the frequency of this solar line is roughly 1.42 GHz [4].

Radio spectral line emissions can be observed in four modes: position switching, frequency switching, beam switching, and On The Fly (OTF) mapping. OTF mapping is a useful observation technique that improves the capabilities of position change. In this technology, the antenna scans across a field smoothly and fast while continually recording spectral data and antenna location information. Unlike previous mapping methodologies that focus on discrete places in the sky, OTF mapping allows a single dish radio telescope to generate maps of small portions of the sky economically and precisely [5]. OTF mapping reduces changes in atmospheric and system parameters, such as antenna pointing and calibration, and increases observing efficiency [6]. There are several basic types of OTF scanning geometries used in radio telescopes, including spiral scanning, hypocycloid scanning, and raster scan approaches. The raster scan approach is the most basic mode of a radio telescope to construct and it operates only in position switched mode. This is used to monitor the antenna's pointing and to measure the flux density on a radio source such as the sun. The sun is an essential natural cosmic laboratory for researching many physical processes that may occur in more distant star objects. Mapping the solar brightness temperature at centimeter and millimeter wavelengths is critical because it allows us to investigate the chromosphere and lower corona layer of the solar atmosphere [7], [8].

The researchers resolved this problem in various published studies, with some of the most significant contributions being the solar higher resolution maps created using a 15-foot diameter millimeter antenna at Aerospace Corp by Simon in 1965 [9]. Additionally, Emerson et al. (1979) developed a

technique for deconvolution of beam switching data into total power images, significantly enhancing our ability to comprehend centimeter and millimeter waves [10]. By 1980, a number of radio telescopes were using beam switching continuum observations. This involves moving the antenna in a two-dimensional raster scan pattern across a certain area of the sky while quickly moving the telescope sub-reflector to get differential measurements of total power. In 1990, a number of radio observations added OTF mapping capabilities for both spectral lines and the continuum [11]-[15]. The RTF radio telescope, created by the institute of applied astronomy and the Russian Academy of Sciences [16], is another method of solar radio mapping carried out with a single dish telescope.

In the last decade, spectral line OTF has been made practicable at a few observatories, and it has been demonstrated to be an effective method. These observatories include the Nobeyama Radio Observatory (NRO) 45 m, and the Atacama Submillimeter Telescope Experiment (ASTE) 10 m [15]. Consequently, the variation of radio astronomical observation techniques leads to improve the communication systems such as Wi-Fi, satellites navigations, global position systems, antennas of phone cells, TV-broadcasting, and all issues of information technology (IT).

In this work, the Baghdad University Radio Telescope (BURT) was utilized which operated at a frequency of 1.42 GHz. BURT has the raster scan technique. This technique is used to construct contour maps the solar intensity and its surrounding area. These contour maps involved the received power, antenna temperature, and solar brightness temperature. These maps were estimated using different window sizes in the sky as interpreted in Section (3). The main objective of this study is to investigate the solar radio emission characteristics of the quiet Sun at 21 cm by analyzing how the observed parameters—received power, antenna temperature, and brightness temperature—vary with scanning window size, and to assess the accuracy and performance of the BURT system for solar spectral observations.

2 THEORETICAL CONCEPTS

The concept of the antenna temperature (T_A) could be defined as the temperature of the antenna radiation resistance, which equal to resistance temperature. T_A could be given by the following equation [16]:

$$T_A = \frac{1}{2k} A_e \iint T_B(\theta,\phi) P(\theta,\phi) d\Omega, \quad (1)$$

where k is Boltzmann constant, A_e is the effective area of the antenna. T_A is equivalent to the convolution between the source brightness temperature $T_B(\theta,\phi)$ with beam power pattern $P(\theta,\phi)$of the radio telescope, were (θ,ϕ) are elevation and azimuth of the antenna respectively. $d\Omega$ is the antenna solid angle.

Using the Nyquist theorem, could be introduce T_A by [16]:

$$\boldsymbol{T_A = \frac{P_A}{kG\Delta v}}, \quad (2)$$

where P_A is the antenna power, G is the antenna gain, and Δv is the bandwidth frequency of the telescope radiometer in Hz.

In the case of the solid angle Ω_s subtended by the source is much larger than the solid angle subtended by the antenna Ω_A; this leading to assume that T_A is exactly equal to T_B. While if the source does not completely fill the beam width i.e. $\Omega_A >> \Omega_s$, so that the measured T_A will be less than T_B, then T_B is given by [17]:

$$T_B = \frac{\Omega_A}{\Omega_s} T_A. \quad (3)$$

3 SCANNING GEOMETRY

The scanning geometry of BURT is the raster scan technique. This technique is used for mapping a square region or window of size (As) in the sky, where the observed source is located in the center of this window (θ_o, ϕ_o). Raster scan moves the antenna within a selected window in a straight line at a fixed elevation where the first line begins from the left bottom of the chosen window. Then each line is segmented by number of points (n) separated in a regular distance, or step size (Δs), while the antenna lies on a certain point, the spectrometer continuously integral the incoming signals of each point. At the finish of the first scanned line, the antenna rises up by (Δs) and return to backward direction scan in the second line, then these steps are repeated until the region is completely mapped. Consequently, the antenna is moved from the starting point (Sp) until to the Finishing point (Fp), as shown in Figure 1.

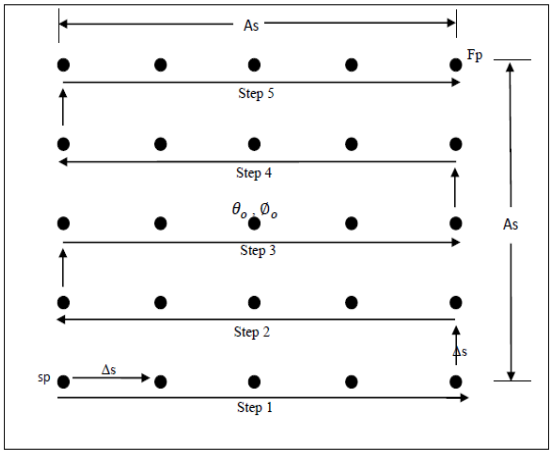

Figure 1: Path of BURT antenna movement in mapping of 25 points as the raster scan.

To verify he results, the root mean square noise (σ) for a total power measurement is computed and given by the following [18]:

$$\sigma = \frac{T_A}{\eta_{spect}\sqrt{\Delta v t_{on}}}\left[1 + \frac{t_{on}}{t_{off}}\right]^{1/2}, \qquad (4)$$

η_{spect} is the spectrometer efficiency and approximately equal to one, Δv is defined in section 2, t_{on} is the required time to record the power of each point, and t_{off} is the spent time to transfer the antenna from point to point.

The optimum t_{off} measurements could be given as [18]:

$$t_{off}^{optimum} = \sqrt{n}\, t_{on}, \qquad (5)$$

n is the total number of scanned points within a selected window.

Then, the total time of the scanning t_{scan} could be given as [18]:

$$\boldsymbol{t_{scan} = t_{off} + n t_{on}}. \qquad (6)$$

Therefore, (4) could be written as [18]:

$$\boldsymbol{\sigma = \frac{T_A}{\eta_{spect}\sqrt{\Delta v t_{scan}}}\left[1 + \frac{1}{\sqrt{n}}\right]} \qquad (7)$$

4 OBSERVATIONS AND RESULTS

The Solar observations are carried out using archive data of Baghdad University Radio Telescope (BURT) with raster scan technique. This telescope has a diameter of 3m (D), its Half Power Beam Width (θ_{HPBW}) is about equal to 4°, and its aperture efficiency (η) is approximately equal to 0.54 [19]. Our observations were carried out from April 3, 2019 to June 4, 2019, which are presented in Table 1.

Table 1: Solar observations using raster scan technique.

Date	Local Time (Am)	As (degree)	Δs (degree)	No. of points (n)=[Integer(A	Spent time (min.)
3-4-2019	10:14	1	0.5	9	3
6-4-2019	10:5	2	1	9	5
13-4-2019	11:10	3	1	16	9
16-4-2019	10:21	4	1	25	15
20-4-2019	11:24	5	1	36	21
23-4-2019	12:06	6	2.5	9	8
27-4-2019	11:05	7	3	9	8
30-4-2019	9:9	8	3	16	13
4-5-2019	9:49	9	3	16	12
4-5-2019	10:20	10	3	9	13

Our results depend on the two cases. In the first, the size window is half of our telescope's beamwidth (i.e. As = $\frac{1}{2}\theta_{HPBW}$), and in the second, the size window is twice our telescope's beamwidth (As = $2\theta_{HPBW}$). Figure 2 shows these two different situations.

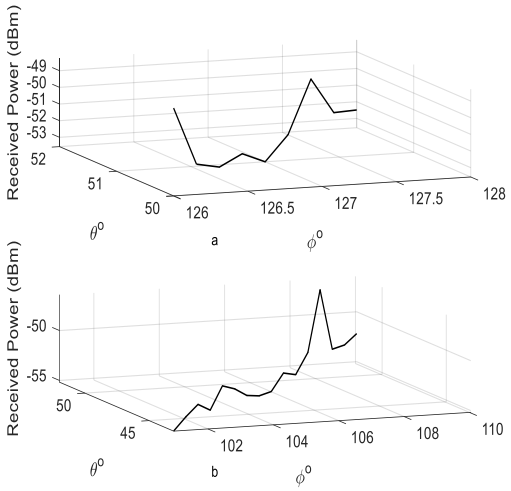

Figure 2: Received power (dBm) as a function of ($\boldsymbol{\phi}$°, $\boldsymbol{\theta}$°), a) As=2°×2°, Δs=1°, b) As=8°×8°, Δs=3°.

It should be noted that in Figure 2a, the recorded signal is shortened since the window size chosen is smaller than the telescope beamwidth, and its terminal is truncated.

The optimum case that have been obtained at As=8°×8°, and Δs=3° (see Fig. 2b), because of that this window size is larger than our telescope beamwidth and enables the antenna to scan this

window by complete shape of the beamwidth, so that the signal is recorded totally as shown in Figure 3. Therefore, the rest computations in this study were dependent on this size As=8°×8°, and Δs=3°.

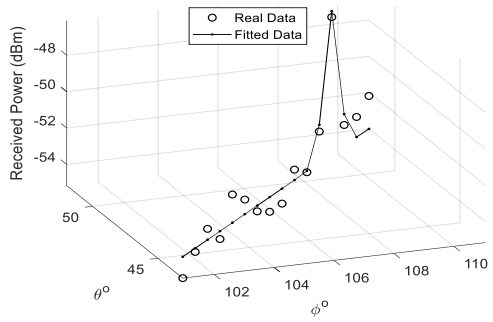

Figure 3: Power received (dBm) as a function ($\phi°$, $\theta°$), and its Gaussian fitting for (As=8°×8°, Δs=3°, and n=16 points).

The quality of goodness fitting is verified using R square criterion [20]:

$$R^2 = \left|1 - \frac{\sum\sum(Fitted\ data - Recieved\ data)^2}{\sum\sum(Fitted\ data - Mean(Recieved\ data))^2}\right|. \quad (8)$$

The optimum value of R that verifies the Gaussian fitting, shown in Figure 4, is found to be 0.78. This value shows high correlation between the observed data and fitted data. Therefore, the fitted data are used in all computations.

The central part of the fitted power is extracted and plotted as a function of antenna position, as shown in Figure 4.

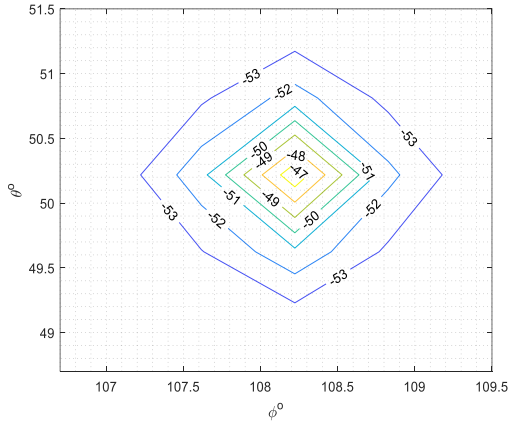

Figure 4: Contour plot of the received fitted power (dBm) as a function of antenna position ($\theta°$, $\phi°$).

The received fitted power is converted to T_A using (2), by setting the Boltezmann constant (k = 1.38×10^{-23} J/K), the bandwidth frequency (dv = 6×10^9 Hz), and the gain (G = 30 dB) the result illustrated in Figure 5.

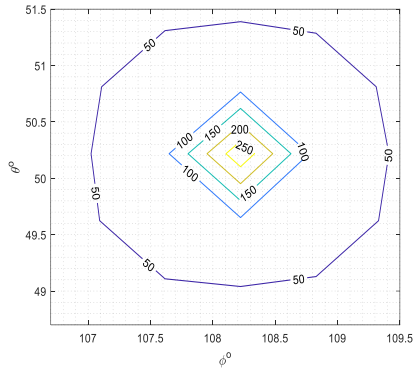

Figure 5: Contour plot of the T_A (K) as a function of antenna position ($\theta°$, $\phi°$) within the window (As=8°×8°, Δs=3).

Also, T_B is computed via (3), by setting $\Omega_A \sim \theta_{HPBW}$, and Ω_s = 0.5°. then the result is displayed as in Figure 6.

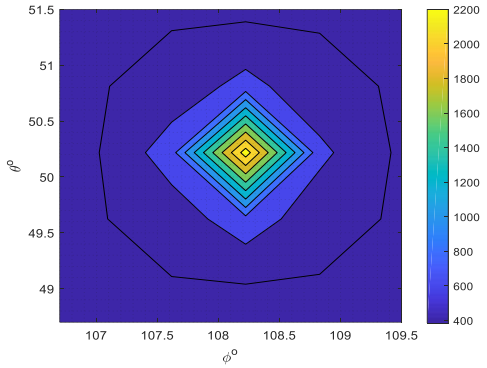

Figure 6: Contour plot of the T_B (K) as a function of antenna position ($\theta°$, $\phi°$) within the window (As=8°×8°, Δs=3).

BURT raster scan mapping technique is limited by two boundaries:

1) The scan time of any observed area should be less than 16 minutes. This time ensure the observed source inside the selected window, due to Earth rotation approximately equal to 1° for each 4 minutes.
2) For large scanned window, the step size (Δs) should be chosen greater than 1°, to ensure the scanned time is not exceeding the required time (16 minutes).

The root mean noise power (σ) is computed via (7) by setting (T_A = 288 K, and η_{spect} =1), as illustrated in Figure 7.

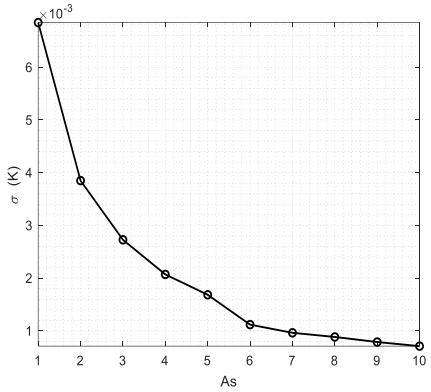

Figure 7: The relationship between σ and As.

It should be pointed here, (As) values (1 to 10), and Δs is taken to equal to one.

4 CONCLUSIONS

In this study, solar radio observations were conducted by the Baghdad University Radio Telescope (BURT) over a two-month period in 2019. This data was observed at the wavelength of 21 cm using the raster scan mapping technique which is considered one of important observation techniques of BURT. This approach enabled us to the construction of solar intensity contour maps and verified the telescope's pointing accuracy. The analysis of the results, showed that window sizes larger than the BURT beamwidth produced the most reliable results because of this window size should be twice the main lobe of BURT (4°). In addition, the maximum received power, antenna temperature, and brightness temperature were computed within large window sizes and found to be −46 dBm, 288 K, and 2300 K, respectively. These values are seemed little values and indicating that the Sun was in a quiet phase of its activity cycle. Furthermore, the root mean square error analysis (σ) is computed to confirm that the 8°×8° window size provided the highest precision, with $\sigma = 1\times10^{-3}$ K. The lesser value is demonstrated the highest accuracy and largest effectiveness of BURT for solar radio observations at 21 cm.

ACKNOWLEDGMENTS

We would like to express our thank and gratitude to the head of the department of Astronomy and Space, academic staff, colleagues and all friends at the College of Science, University of Baghdad for their valuable advices and encouragement.

REFERENCES

[1] S. Costanzo and Di Massa, "Near-field to far-field transformation with planar spiral scanning," Progress In Electromagnetics Research, vol. 73, pp. 49-59, 2007.

[2] T. Yang, "The frequency of hydrogen emission from the Sun," Wabash Journal of Physics, vol. 4, pp. 1-6, 2016.

[3] R. J. Maddalena, "Reduction and analysis techniques," in Single-Dish Radio Astronomy: Techniques and Applications, ASP Conference Series, vol. 278, pp. 329-352, 2002.

[4] J. M. Dickey, "Spectral line advanced topics," in Single-Dish Radio Astronomy: Techniques and Applications, ASP Conference Series, vol. 278, pp. 209-225, 2002.

[5] A. Pellizzoni, F. Buffa, E. Egron, M. Iacolina, S. Loru, A. Maccaferri, G. Murtas, A. Navarrrini, A. Orfei, S. Righini, G. Serra, G. Valente, A. Zanichelli, P. Zucca, and M. Messerotti, "High resolution imaging of the solar chromosphere in the centimetre-millimetre band through single-dish observations," in 2nd URSI AT-RASC, Gran Canaria, May 28–June 1, 2018.

[6] I. Boothroyd, K. Blagrave, F. J. Lockman, P. G. Martin, D. Goncalves, and S. Srikkanth, "Accurate galactic 21-cm HI measurements with NRAO Green Bank Telescope," Astronomy & Astrophysics, vol. 536, pp. 1-23, 2001.

[7] D. Buhl and A. Tlamicha, "The mapping of the Sun at 3.5 mm," Astronomy & Astrophysics, vol. 5, pp. 102-112, 1970.

[8] D. T. Emerson, U. Klein, and C. G. Haslam, "A multiple beam technique for overcoming atmospheric limitations to single-dish observations of extended radio source," Astronomy & Astrophysics, vol. 76, pp. 92-105, 1979.

[9] D. T. Emerson and R. Grave, "The reduction of scanning noise in raster scanned data," Astronomy & Astrophysics, vol. 190, pp. 353-358, 1988.

[10] J. G. Mahgum, D. T. Emerson, and E. W. Greisen, "The on-the-fly imaging technique," Astronomy & Astrophysics, vol. 474, no. 2, pp. 679-687, 2007.

[11] N. Goplaswamy, S. M. White, and M. R. Kundu, "Large scale features of the Sun at 20 centimeter wavelength," The Astrophysical Journal, vol. 379, pp. 366-380, 1991.

[12] J. G. Mahgum, D. T. Emerson, and E. W. Greisen, "The on-the-fly imaging technique," in Imaging at Radio through Submillimeter Wavelengths, ASP Conference Series, vol. 17, 2000.

[13] M. Loukitcheva and V. G. Nagnibeda, "Radio emission of solar chromosphere at millimeter wavelength," in Proc. 1st Solar & Space Weather Euro Conference, Spain, Sep. 25-29, 2000.

[14] A. Ipotova, A. G. Mikhailov, V. V. Mardyshkin, and M. A. Kharinov, "Mapping the Sun with RTF-32 radio telescopes," Solar System Research, vol. 40, no. 2, pp. 169-173, 2006.

[15] T. Sawada, N. Ikeda, K. Sunda, N. Kuno, T. Kamazaki, K. Morita, Y. Kurono, N. Koura, N. Abe, S. Kawase, J. Maekawa, O. Horigome, and K. Yanagisawa, "On-the-fly observing system of the Nobeyama 45-m and ASTE 10-m telescopes," Publications of the Astronomical Society of Japan, vol. 60, pp. 445-455, 2008.

[16] G. F. Wong, S. Horiuchi, G. A. Green, N. F. Tothill, and K. Sugimoto, "Implementation of Tidbinbilla 70-m on-the-fly mapping and hydrogen radio recombination line early results," Monthly Notices of the Royal Astronomical Society, vol. 458, no. 1, pp. 151-157, 2016.

[17] K. O'Neil, "Single dish calibration techniques at radio wavelengths," in NAIC/NRAO School on Single Dish Radio Astronomy, ASP Conference Series, 2002, pp. 1-18.

[18] H. Ungerechts, W. Brunswig, C. Kramer, G. Paubert, A. Sievers, and W. Wild, "Spectral-line on-the-fly at IRAM 30 m telescope," in Imaging at Radio through Submillimeter Wavelengths, ASP Conference Series, vol. 17, pp. 179-189, 2000.

[19] U. E. Jallod, H. S. Mahdi, L. T. Ali, and K. M. Abood, "The impact of partial solar eclipse on the observation of neutral hydrogen emission line," Iraqi Journal of Science, vol. 65, no. 10, pp. 6079-6087, 2024.

[20] M. S. Doulah, "Robust coefficients of determination: A measure of goodness of fit," International Journal of Scientific and Engineering Research, vol. 4, no. 5, pp. 1715-1717, 2013.